Structural Engineering and Mechanics, Vol. 5, No. 4 (1997) 471-490
DOI: http://dx.doi.org/10.12989/sem.1997.5.4.471

The patch tests and convergence for nonconforming Mindlin plate bending elements

Yong-Myung Park†

Steel Structure Technology Division, Research Institute of Industrial Science and Technology, Seoul 135-777, Korea

Chang-Koon Choi‡

Department of Civil Engineering, Korea Advanced Institute of Science and Technology, Taejon 305-701, Korea

Abstract. In this paper, the classical Irons' patch tests which have been generally accepted for the convergence proof of a finite element are performed for Mindlin plate bending elements with a special emphasis on the nonconforming elements. The elements considered are 4-node and 8-node quadrilateral isoparametric elements which have been dominantly used for the analyses of plate bending problems. It was recognized from the patch tests that some nonconforming Mindlin plate elements pass all the cases of patch tests even though nonconforming elements do not preserve conformity. Then, the clues for the Mindlin plate element to pass the Irons' patch tests are investigated. Also, the convergent characteristics of some nonconforming Mindlin plate elements that do not pass the Irons' patch tests are examined by weak patch tests. The convergence tests are performed on the benchmark numerical problems for both nonconforming elements which pass the patch tests and which do not. Some conclusions on the relationship between the patch test and convergence of nonconforming Mindlin plate elements are drawn.

Key words: nonconforming Mindlin plate element; Irons' patch tests; weak patch test; convergence requirement.

1. Introduction

In the past few decades, a lot of research efforts in the development of Mindlin plate elements have been directed at avoiding shear-locking problems and also at improving the performance in a coarser mesh, thus rendering them effective and reliable for thin plate/shell applications. As a way to accomplish the objective, the research in the nonconforming finite elements has drawn interests of a number of finite element analysts because these elements generally show an improved performance than conforming counterparts (Choi and Schnobrich 1975, Taylor, *et al.* 1976, Choi and Kim 1989, Choi and Park 1989, Kim and Choi 1992).

To ensure the convergence of a finite element, it is necessary for the interpolation functions to fulfill the completeness criteria. The patch test which has been generally accepted for the

† Senior Researcher
‡ Professor

convergence proof of a finite element was first introduced by Irons, *et al.* as a part of the development of a set of plate bending elements to check that the incompatible Kirchhoff plate bending element can reproduce a state of constant strain (Bazeley, *et al.* 1966, Irons and Razzaque 1972). A lot of studies on the theory and practice of the test were followed after Irons' initial work. Razzaque (1986) suggested that an element must pass the patch test to converge. Taylor, *et al.*(1986) reported that the patch test is the necessary and sufficient condition for the convergence of solution and also suggested the concept of weak patch test where the constant strain condition need not be satisfied exactly at the initial stage but should be satisfied at the limit as the patch size tends to zero. Belytschko and Lasly (1988) suggested a 'fractal' patch test which uses a sequence of distorted meshes where the initial distorted patch structure is successively refined by fractal refinement. Even though some researchers are suspicious if passing the patch test can guarantee the convergence, (Verma and Melosh 1987, Stummel 1980) it still remains as a valuable tool for the finite element convergence test and as a debugging aid.

In this study, the patch tests for Mindlin plate bending elements with a special emphasis on the nonconforming 4-node and 8-node elements are presented. The nonconforming elements generally violate the interelement continuity of displacements because of the addition of higher modes to the basis element. Therefore, it is desirable to investigate the convergence of the nonconforming type elements by the patch tests.

The clues to pass the standard patch tests for the nonconforming Mindlin plate elements are investigated to the depth in this study. For the nonconforming elements which fail to pass the Irons' patch test, the weak patch tests are also performed to examine the convergent characteristics of the elements. Then, the convergence tests are performed on the benchmark numerical problems for both nonconforming elements which pass the patch tests and which do not. Some conclusions on the convergence requirement of nonconforming Mindlin plate elements are drawn from these numerical results.

2. Formulation of nonconforming Mindlin plate element

In the Mindlin plate shown in Fig. 1, the displacement fields, i.e., the transverse displacement w and two rotations α and β, are assumed by the same shape functions as follows.

$$\begin{Bmatrix} w \\ \alpha \\ \beta \end{Bmatrix} = \sum_{i=1}^{n} N_i \begin{Bmatrix} w_i \\ \alpha_i \\ \beta_i \end{Bmatrix} \tag{1}$$

where, n is the number of nodes in an element. The shape functions N_i for quadrilateral elements are easily found in the published literatures (Bathe 1982). The curvature and shear strain components are then given by the following equations.

$$\chi = \begin{Bmatrix} \chi_x \\ \chi_y \\ \chi_{xy} \end{Bmatrix} = \begin{Bmatrix} -\partial\alpha/\partial x \\ -\partial\beta/\partial y \\ -(\partial\alpha/\partial y + \partial\beta/\partial x) \end{Bmatrix} = \boldsymbol{B}_b \boldsymbol{u} \tag{2a}$$

$$\gamma = \begin{Bmatrix} \gamma_x \\ \gamma_y \end{Bmatrix} = \begin{Bmatrix} \partial w/\partial x - \alpha \\ \partial w/\partial y - \beta \end{Bmatrix} = \boldsymbol{B}_s \boldsymbol{u} \tag{2b}$$

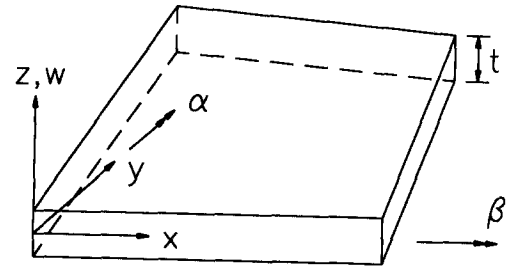

Fig. 1 Degrees of freedom for Mindlin plate.

where, $\boldsymbol{B}_b$ is the bending strain matrix, $\boldsymbol{B}_s$ is the shear strain matrix, and $\boldsymbol{u}$ is the nodal displacement vector $\{w_i, \alpha_i, \beta_i\}^T$. Then, the element stiffness matrix $\boldsymbol{K}_e$ is obtained in the following form.

$$\boldsymbol{K}_e = \int_V \boldsymbol{B}_b^T \boldsymbol{D}_b \boldsymbol{B}_b \, dV + \int_V \boldsymbol{B}_s^T \boldsymbol{D}_s \boldsymbol{B}_s \, dV \tag{3}$$

where, $\boldsymbol{D}_b$ and $\boldsymbol{D}_s$ are material matrices for the bending and shear rigidity.

It is well known that the isoparametric Mindlin plate bending element, when the stiffness matrix of the element in Eq. (3) is formed by the normal Gaussian integration, shows a poor accuracy of solution especially in low order element. This is associated with the evaluation of incorrect shear strain which makes an element too stiff in a bending mode.

The major schemes suggested to remedy these problems are: 1) the addition of nonconforming displacement modes (Choi and Schnobrich 1975, Taylor, *et al.* 1976, Choi and Kim 1989, Choi and Park 1989, Kim and Choi 1992); 2) the reduced (selectively) integration (Zienkiewicz, *et al.* 1971, Pugh, *et al.* 1978); and 3) the construction of the substitute shear strain fields (Hinton and Huang 1986, Donea and Lamain 1987). For the development of appropriate Mindlin plate elements, the first remedy, i.e, addition of nonconforming modes, enriches the interpolation functions with higher modes whereas the latter two techniques lead to lowering the order of shape function for the representation of shear strains.

In formulation of the nonconforming elements, it is desirable that the nonconforming displacement modes are of the same form as the errors or what are missing in the original displacement approximation. Thus, the actual displacement field can be better approximated by the addition of nonconforming displacement modes and can be expressed as

$$u' = \sum N_i u_i + \sum \bar{N}_i \bar{u}_i \tag{4}$$

where, N_i = original conforming shape function, $\bar{N}_i$ = nonconforming modes, u_i = original nodal displacement components, and $\bar{u}_i$ = additional unknowns corresponding to the nonconforming modes.

Then, the enlarged force-displacement equation is formulated by direct application of the principle of minimum potential energy and obtained as

$$\begin{bmatrix} \boldsymbol{K}_{cc} & \boldsymbol{K}_{cn} \\ \boldsymbol{K}_{cn}^T & \boldsymbol{K}_{nn} \end{bmatrix} \begin{Bmatrix} \boldsymbol{u} \\ \bar{\boldsymbol{u}} \end{Bmatrix} = \begin{Bmatrix} \boldsymbol{F} \\ 0 \end{Bmatrix} \tag{5}$$

where, subscript c denotes conforming and n nonconforming part, respectively, and each submatrix is defined as follows.

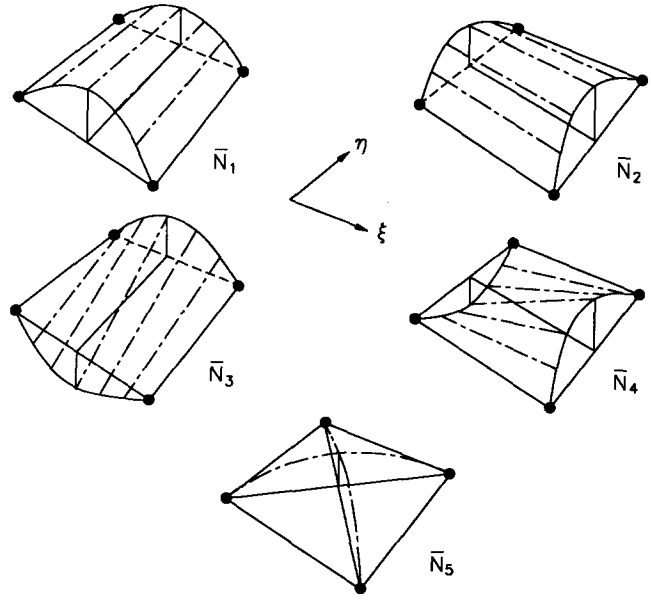

Fig. 2 Nonconforming displacement modes for 4-node element.

$$\begin{aligned} \boldsymbol{K}_{cc} &= \int_V \boldsymbol{B}^T \boldsymbol{D}\boldsymbol{B} dV \\ \boldsymbol{K}_{cn} &= \int_V \boldsymbol{B}^T \boldsymbol{D}\bar{\boldsymbol{B}} dV \\ \boldsymbol{K}_{nn} &= \int_V \bar{\boldsymbol{B}}^T \boldsymbol{D}\bar{\boldsymbol{B}} dV \end{aligned} \tag{6}$$

In Eq. (5), $\boldsymbol{F}$ means the physical nodal force vector and the null vector $\mathbf{0}$ in the lower part of the load vector indicates that no nodal loads can be applied in association with the nonconforming modes. In Eq. (6), $\boldsymbol{B}$ and $\bar{\boldsymbol{B}}$ denote strain matrices by conforming and nonconforming parts, respectively.

The enlarged element stiffness matrix in Eq. (5) can be condensed back to the same size of stiffness matrix of the original conforming elements. The modified set of equations now becomes

$$(\boldsymbol{K}_{cc} - \boldsymbol{K}_{cn}\boldsymbol{K}_{nn}^{-1}\boldsymbol{K}_{cn}^T)\boldsymbol{u} = \boldsymbol{F} \tag{7}$$

The nonconforming displacement modes for a 4-node element are shown in Fig. 2 and the polynomial functions are as follows.

$$\begin{aligned} \bar{N}_1 &= (1-\xi^2) \\ \bar{N}_2 &= (1-\eta^2) \\ \bar{N}_3 &= \eta(1-\xi^2) \\ \bar{N}_4 &= \xi(1-\eta^2) \\ \bar{N}_5 &= (1-\xi^2)(1-\eta^2) \end{aligned} \tag{8}$$

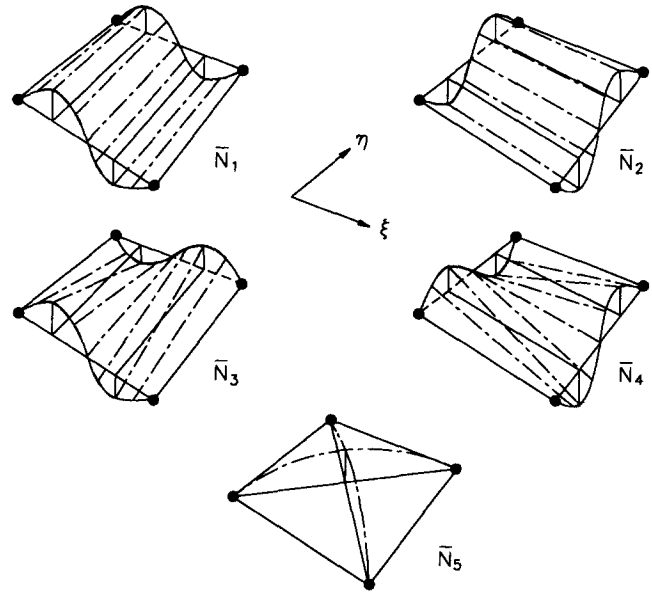

Fig. 3 Nonconforming displacement modes for 8-node element.

Similarly, the nonconforming displacement modes for 8-node element are shown in Fig. 3 and the polynomial functions are as follows.

$$\begin{aligned}
\bar{N}_1 &= \xi(1-\xi^2) \\
\bar{N}_2 &= \eta(1-\eta^2) \\
\bar{N}_3 &= \xi\eta(1-\xi^2) \\
\bar{N}_4 &= \xi\eta(1-\eta^2) \\
\bar{N}_5 &= (1-\xi^2)(1-\eta^2)
\end{aligned} \tag{9}$$

The first two modes in Eqs. (8) and (9) are to enhance the flexural behavior and the third and the fourth modes contribute to soften the twisting behavior. The fifth mode adds the bubble shape displacement in the element. Selective combinations of the nonconforming displacement modes defined in the Eqs. (8) and (9) are possible to form various types of nonconforming elements.

Based on the previous development of efficient nonconforming Mindlin plate bending elements, the notable 4-node elements are listed in Table 1 and 8-node elements in Table 2 together with conforming counterparts (Choi and Schnobrich 1975, Choi and Kim 1989, Choi and Park 1989, Kim and Choi 1992). In the Tables 1 and 2, the first character '*C*' indicates the original conforming (isoparametric) element and '*NC*' denotes nonconforming element. The integration orders in Tables 1 and 2 for the evaluation of bending and shear stiffness are the minimum orders required to avoid the zero-energy modes.

3. The patch tests

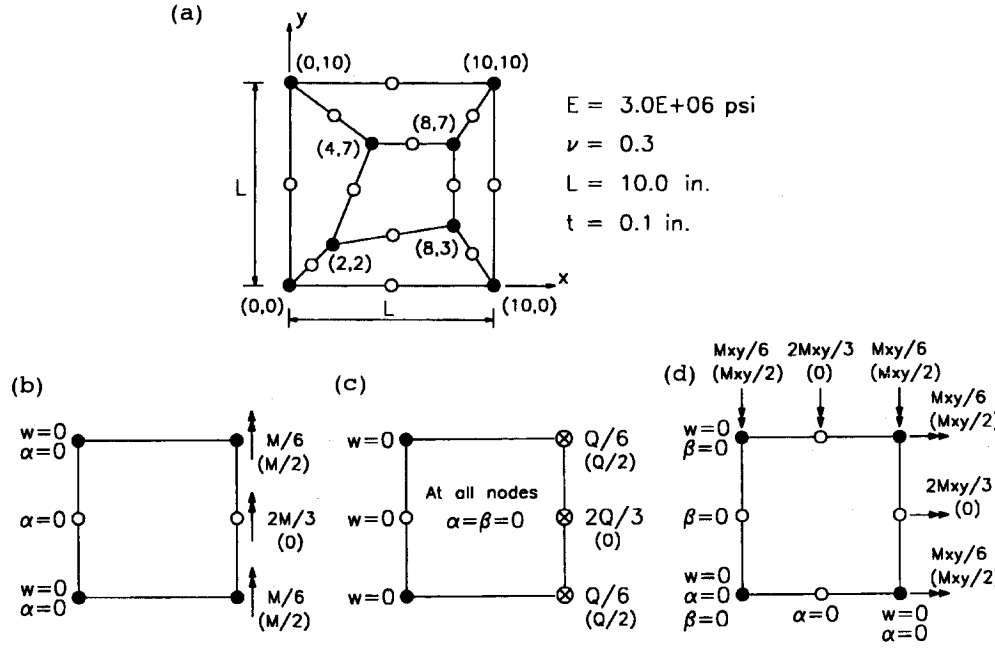

O: Nodes for 8-node element only, ( ): Loading for 4-node element

Fig. 4 Patch tests; (a) Configuration of model, (b) Pure bending, (c) Pure shearing, (d) Pure Twisting.

Table 1 Designation and patch test results for 4-node elements

Designation	Nonconforming modes		Integration order		Patch test		
	w	α, β	K_b	K_s	Bending	Shearing	Twisting
C4	–	–	2	2	Fail†	Pass	Fail†
NC4-A1	$\bar{N}_5$	–	2	2	Fail	Pass	Fail
NC4-A2	–	$\bar{N}_5$	2	2	Fail	Fail	Fail
NC4-A3	$\bar{N}_5$	$\bar{N}_5$	2	2	Fail	Fail	Fail
NC4-B0	$\bar{N}_1$, $\bar{N}_2$	–	2	2	Fail‡	Fail‡	Fail‡
NC4-B1	$\bar{N}_1$, $\bar{N}_2$, $\bar{N}_5$	–	2	3	Fail‡	Fail‡	Fail‡
NC4-B2	$\bar{N}_1$, $\bar{N}_2$	$\bar{N}_5$	2	2	Fail‡	Fail†	Fail‡
NC4-B3	$\bar{N}_1$, $\bar{N}_2$, $\bar{N}_5$	$\bar{N}_5$	2	3	Fail‡	Fail†	Fail‡
NC4-C0	$\bar{N}_1 \sim \bar{N}_4$	–	2	2	Pass	Fail※	Pass
NC4-C1	$\bar{N}_1 \sim \bar{N}_5$	–	2	3	Pass	Fail※	Pass
NC4-C2	$\bar{N}_1 \sim \bar{N}_4$	$\bar{N}_5$	2	2	Pass	Fail※	Pass
NC4-C3	$\bar{N}_1 \sim \bar{N}_5$	$\bar{N}_5$	2	3	Pass	Fail※	Pass

† pass the weak patch test (WPT) in thick plate only
‡ pass WPT in thick and thin plate
※ do not pass WPT in thick and thin plate

The methodology for the patch tests is found in a number of published materials (Bathe 1982, Hinton and Huang 1986). In the plate bending problem, the patch test should be carried out for three cases of pure stress/strain states, namely, the pure bending, pure shearing, and

Table 2 Designation and patch test results for 8-node elements

Designation	Nonconforming modes		Integration order		Patch test		
	w	α, β	K_b	K_s	Bending	Shearing	Twisting
C8	–	–	3	2	Fail‡	Pass	Fail‡
NC8-A1	$\bar{N}_5$	–	2	3	Pass	Pass	Pass
NC8-A2	–	$\bar{N}_5$	3	2	Fail‡	Fail†	Fail‡
NC8-A3	$\bar{N}_5$	$\bar{N}_5$	3	3	Pass	Fail†	Pass
NC8-AS[1]	$\bar{N}_3, \bar{N}_4, \bar{N}_5$	–	2	3	Pass	Pass	Pass
NC8-BS[1]	$\bar{N}_5$	–	2	3	Pass	Pass	Pass
NC8-CS[1]	$\bar{N}_1, \bar{N}_2, \bar{N}_5$	–	2	3	Pass	Pass	Pass
NC8-DS[1]	$\bar{N}_1 \sim \bar{N}_5$	–	2	3	Pass	Pass	Pass
NC8-QH[2]	–	$\bar{N}_1, \bar{N}_2, \bar{N}_5$	3	2	Fail‡	Fail†	Fail‡

1): Choi and Kim 1989.
2): Kim and Choi 1992.
† pass the weak patch test (WPT) in thick plate only
‡ pass WPT in thick and thin plate

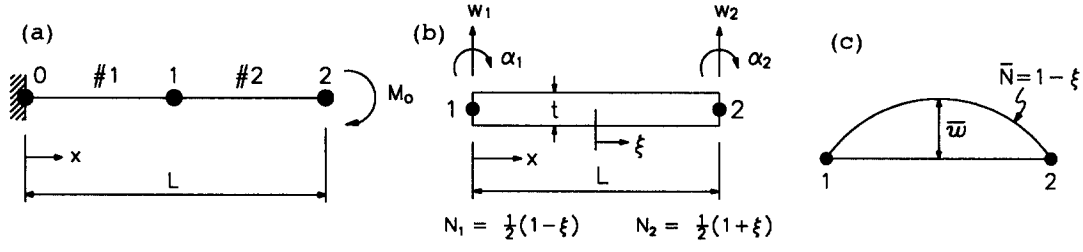

Fig. 5 Beam analogue; (a) Cantilever beam subject to end moment, (b) Linear beam element, (c) Nonconforming mode.

pure twisting cases. Patch test models with the meshes of arbitrary quadrilaterals and the loading features for the three conditions are shown in Fig. 4.

The patch test results for the 4-node conforming and nonconforming Mindlin plate elements are listed in Table 1, and 8-node elements in Table 2. As recognized in the tables, the original isoparametric conforming elements, C4 and C8, do not pass the Irons' patch tests except for the pure shearing case, whereas some of the nonconforming 8-node elements, such as NC8-AS through NC8-DS, pass all the three pure stress cases.

3.1. Pure bending

The clues to pass the pure bending test depicted in Fig. 4(b) will be explained by beam analogue. Consider a cantilever beam which consists of two linear elements and is subjected to a bending moment at its end as shown in Fig. 5(a). In the situation, the cantilever beam is in the state of pure bending and the exact solutions for transverse displacement and rotation are as follows.

$$w_{\text{exact}} = \frac{M_o}{2EI} x^2, \qquad \alpha_{\text{exact}} = \frac{M_o}{EI} x \tag{10}$$

The transverse shear strain γ_x in Eq. (2b) of the #2 element ($x=L/2\sim L$) as shown in Fig. 5(b), for example, is obtained as follows.

$$\gamma_x=\frac{3}{4}\left(\frac{M_oL}{EI}\right)-\left(\frac{3}{4}\frac{M_oL}{EI}+\xi\frac{M_oL}{4EI}\right) \tag{11}$$

where,

$$\frac{\alpha\xi}{\partial x}=\frac{4}{L},\quad w_1=\frac{M_oL^2}{8EI},\quad w_2=\frac{M_oL^2}{2EI},\quad \alpha_1=\frac{M_oL}{2EI},\quad \alpha_2=\frac{M_oL}{EI} \tag{11a}$$

From Eq. (11), if the normal Gauss integration (i.e., a two-point integration) is applied to evaluate the shear stiffness, the transverse shear strains could never be zero at $\xi=\pm 1/\sqrt{3}$ whereas the actual transverse shear strain should be zero in the pure bending state. Therefore, the pure bending situation of the original linear beam element can not be properly represented.

If a nonconforming displacement mode, $\bar{N}=1-\xi^2$ in Fig. 5(c), is added to the transverse displacement field of the bilinear element, the new displacement is defined as

$$w'=(N_1w_1+N_2w_2)+\bar{N}\bar{w} \tag{12}$$

and the transverse shear strain is now obtained as

$$\gamma_x=\left(\frac{3}{4}\frac{M_oL}{EI}+(-\xi)\frac{8}{L}\bar{w}\right)-\left(\frac{3}{4}\frac{M_oL}{EI}+\xi\frac{M_oL}{4EI}\right) \tag{13}$$

The expression in the first parenthesis of the right hand side in Eq. (13) is $\partial w'/\partial x$ and the second is α which is unchanged. In case of $\bar{w}=-M_oL^2/32EI$, the transverse shear strain in Eq. (13) becomes zero irrespective of the location of integration point ξ.

The observation on the beam analogue reveals two facts for a Mindlin plate element to represent pure bending state; (1) the transverse displacement field should be complete to the quadratic order. (2) the polynomial terms remaining after differentiation of transverse displacement, i.e., $\partial w/\partial x$ and $\partial w/\partial y$, should envelope the polynomial terms appeared in the expression for the rotations α and β. These facts mean that the incorrect shear in Mindlin plate elements must be removed properly not to prohibit pure bending behavior of the elements by matching the polynomial terms of $\partial w/\partial x$ (and $\partial w/\partial y$) and those of α (and β), eventually rendering the shear strains to be zero.

In the original isoparametric 4-node element (C4 in Table 1), the transverse displacement field is incomplete to the quadratic order due to the missing terms $\langle\xi^2, \eta^2\rangle$. Also, for the representation of shear strain γ_x, the polynomial terms stemming from $\partial w/\partial x$ contain $\langle 1, \xi, \eta\rangle$ whereas the rotation α contains $\langle 1, \xi, \eta, \xi\eta\rangle$ and similar situation occurs for $\gamma_y(=\partial w/\partial y-\beta)$. Then, the polynomial terms $\langle\xi^2\eta, \xi\eta^2\rangle$ which are necessary to produce the term $\langle\xi\eta\rangle$ after differentiation are absent in the expression for the transverse displacement field of C4 element. It is, therefore, necessary to complement the four terms $\langle\xi^2, \eta^2, \xi^2\eta, \xi\eta^2\rangle$ into the transverse displacement for the 4-node element to pass the patch test for the pure bending state.

In the case of original 8-node element (C8 in Table 2), for the representation of γ_x, the polynomial stemming from $\partial w/\partial x$ contains the terms $\langle 1, \xi, \eta, \xi^2, \xi\eta, \eta^2\rangle$ whereas the polynomial terms $\langle 1, \xi, \eta, \xi^2, \xi\eta, \eta^2, \xi^2\eta, \xi\eta^2\rangle$ are included in the expression of rotation α and a similar problem also occurs for γ_y. The former, which is an expression of the transverse displacement field of C8 element, is complete to the quadratic order, and thus $\langle\xi^2\eta^2\rangle$ is the only term absent

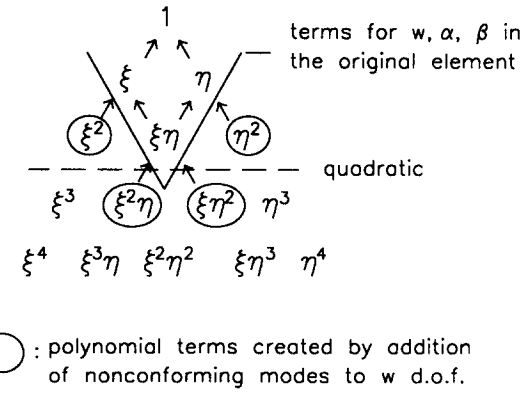

Fig. 6 Polynomial terms stemming from $\partial w/\partial x$ or $\partial w/\partial y$ and rorational degrees of freedom (4-node).

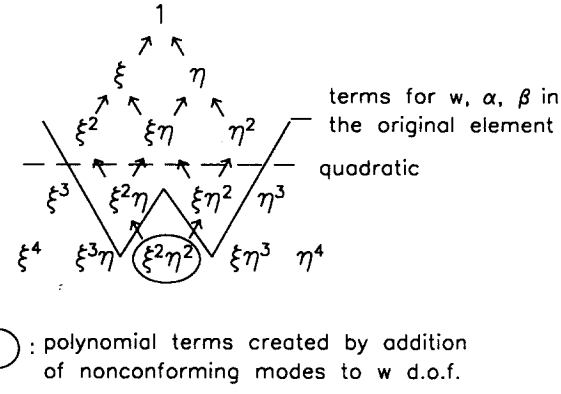

Fig. 7 Polynomial terms stemming from $\partial w/\partial x$ or $\partial w/\partial y$ and rorational degrees of freedom (8-node).

in $\partial w/\partial x$ and $\partial w/\partial y$ for the representation of pure bending.

Such defective problems in C4 and C8 elements can be solved by enhancing the polynomial order of the transverse displacement field. The systematic views are shown in Figs. 6 and 7 for 4-node and 8-node elements, respectively. To compensate the missing terms in the transverse displacement fields, addition of higher order modes is one of the possible means.

For the 4-node nonconforming elements, the nonconforming modes $\bar{N}_1$ and $\bar{N}_2$ in Eq. (8) contain the terms $\langle \xi^2, \eta^2 \rangle$ and the modes $\bar{N}_3$ and $\bar{N}_4$ contain the terms $\langle \xi^2\eta, \xi\eta^2 \rangle$, respectively. The fifth mode $\bar{N}_5$ provides the term $\langle \xi^2\eta^2 \rangle$. The NC4-A$i$($i$=1, 3) series elements which have $\bar{N}_5$ mode in the transverse displacement, do not possess any of the required terms $\langle \xi^2, \eta^2, \xi^2\eta, \xi\eta^2 \rangle$. The NC4-B$i$($i$=0~3) series elements which have $\bar{N}_1$ and $\bar{N}_2$ modes (and $\bar{N}_5$ for NC4-B1 and NC4-B3) in the transverse displacement, possess the terms $\langle \xi^2, \eta^2 \rangle$ but lack the terms $\langle \xi^2\eta, \xi\eta^2 \rangle$. Therefore, NC4-A$i$ and NC4-Bi series elements do not pass the patch test for pure bending case. On the other hand, the NC4-Ci(i=0~3) series elements which have $\bar{N}_1$, $\bar{N}_2$, $\bar{N}_3$, and $\bar{N}_4$ modes (and $\bar{N}_5$ for NC4-C1 and NC4-C3) in the transverse displacement, possess all of the required terms $\langle \xi^2, \eta^2, \xi^2\eta, \xi\eta^2 \rangle$ to pass the patch test for pure bending case as stated earlier.

For the 8-node nonconforming elements, NC8-Ai series elements and NC8-AS through NC8-DS which have $\bar{N}_5$ modes in transverse displacement field pass the pure bending test since

this mode complements the term $\langle \xi^2 \eta^2 \rangle$. However, the NC8-A2 and NC8-QH elements do not pass the pure bending case because these elements do not have the $\bar{N}_5$ modes in the transverse displacement field and thus lack the term $\langle \xi^2 \eta^2 \rangle$.

3.2. Pure shearing

As noticed in Tables 1 and 2, the original isoparametric elements C4 and C8 pass the patch test for the pure shearing case. For the pure shearing condition shown in Fig. 4(c), all the rotational degrees of freedom are supressed and only the transverse degrees of freedom remain active. Recognizing that the transverse deflection is linearly distributed along the horizontal axis, if the shape function for transverse displacement field contains the bilinear terms $\langle 1, \xi, \eta, \xi\eta \rangle$, it is sufficient for a Mindlin plate element to represent the constant shear strain state. This is clearly seen for the conforming C4 and C8 elements.

From Tables 1 and 2, it is also recognized that nonconforming elements for which the nonconforming modes are added to the rotational degrees of freedom do not pass the test for the pure shearing case. As shown in Eqs. (2a) and (2b), the rotational degrees of freedom α and β take part in both the bending strains and shear strains. Therefore, addition of nonconforming displacement modes to rotational degrees of freedom cause the coupling of bending and shear strains in the formulations of the submatrix $\boldsymbol{K}_{cn}$ defined in Eq. (6) and manipulated in Eq. (A.3) in Appendix. The coupling of shear behavior with the bending behavior may cause the contamination and disturbance of the pure shearing situation.

On the other hand, when nonconforming modes are added to the transverse displacement field only (e.g., NC4-A1, NC4-B0, etc. in Table 1), the matrix $\boldsymbol{K}_{cn}$ possesses the shear rigidity only as shown in Eq. (A.4) in Appendix.

In the case of 4-node element, addition of nonconforming modes in Eq. (8) to the transverse displacement field may contaminate the bilinear terms $\langle 1, \xi, \eta, \xi\eta \rangle$ of conforming shape functions. The nonconforming modes $\bar{N}_1$, $\bar{N}_2$, $\bar{N}_3$, $\bar{N}_4$, and $\bar{N}_5$ in Fig. 2 contain the polynomial terms $\langle \xi^2, \eta^2, \xi^2\eta, \xi\eta^2, \xi^2\eta^2 \rangle$ as the highest order term of the polynomial and the derivatives of these modes (i.e., $\partial\bar{w}/\partial x$ or $\partial\bar{w}/\partial y$) yield $\langle \xi \rangle$, $\langle \eta \rangle$, $\langle \xi^2, \xi\eta \rangle$, $\langle \xi\eta, \eta^2 \rangle$, and $\langle \xi^2\eta, \xi\eta^2 \rangle$ from $\bar{N}_1$, $\bar{N}_2$, $\bar{N}_3$, $\bar{N}_4$, and $\bar{N}_5$, respectively. These terms are coupled with the original conforming parts in the matrix $\boldsymbol{K}_{cn}$ as shown in Eq. (A.4). Therefore, the nonconforming 4-node elements with any of the $\bar{N}_1$, $\bar{N}_2$, $\bar{N}_3$, $\bar{N}_4$ modes which produce the bilinear terms after differentiation of transverse displacement, failed in the patch test for the pure shearing case while the NC4-A1 element with $\bar{N}_5$ mode which does not produce any bilinear term passes the patch test.

For the 8-node element, the nonconforming modes $\bar{N}_1$, $\bar{N}_2$, $\bar{N}_3$, $\bar{N}_4$, and $\bar{N}_5$ in Eq. (9) contain the polynomial terms $\langle \xi^3, \eta^3, \xi^3\eta, \xi\eta^3, \xi^2\eta^2 \rangle$ as the highest order term of the polynomial, respectively, and the derivatives of these modes yield $\langle \xi^2 \rangle$, $\langle \eta^2 \rangle$, $\langle \xi^3, \xi^2\eta \rangle$, $\langle \xi\eta^2, \eta^3 \rangle$, and $\langle \xi^2\eta, \xi\eta^2 \rangle$ from $\bar{N}_1$, $\bar{N}_2$, $\bar{N}_3$, $\bar{N}_4$, and $\bar{N}_5$, respectively. Thus, these nonconforming modes which do not produce linear terms after differentiation of the transverse displacement do not contaminate the original conforming linear filelds and thus the pure shearing situation is preserved in the case of 8-node element.

When the nonconforming modes are added to transverse displacement field, the 8-node nonconforming elements (NC8-A1, NC8-AS through NC8-DS) pass the test for pure shearing case, but most of 4-node nonconforming elements except NC4-A1 failed to pass. It will be seen in the convergence test if the elements which did not pass the patch test for the pure shearing

case can converge to the exact solution.

3.3. Pure twisting

The patch test results for the pure twisting case are the same as those for the pure bending case as shown in Tables 1 and 2. In the pure twisting condition, two adjacent edges are simply supported and the distributed tangential edge moments with a constant intensity are applied along the opposite edges as shown in Fig. 4(d). For the situation, only the curvature defined as $\partial\beta/\partial x+\partial\alpha/\partial y$ in Eq. (2a) is non-zero and all other components including the transverse shear strains are zeros. This situation is similar to the pure bending case where the transverse shear strain is zero and the curvatures in each direction ($\partial\alpha/\partial x$ or $\partial\beta/\partial y$) are constants. Therefore, a Mindlin plate element which can represent the pure bending behavior by raising the polynomial order of the transverse displacement field to remove the incorrect shear as described earlier passes the pure twisting test.

4. Weak patch tests

Among a number of finite elements which do not pass exactly the classical Irons' patch test, many of these elements are still reportedly convergent (Kim and Choi 1992, Hughes and Cohen 1978). As will be shown herein, this is true for nonconforming elements as well as isoparametric conforming Mindlin plate bending elements.

The weak patch test is accepted as a tool to relax the strict Irons' patch test for convergence proof (Taylor, *et al.* 1986, Belytshko and Lasly 1988). In the test, the errors in the displacement and those in the stress should diminish as the mesh is progressively refined. The former can be evaluated by comparion with the exact displacement and the latter by means of the energy norm which measures the stress error.

Elements C4, NC4-Bi(i=1~3), NC4-B2, and NC4-Ci(i=0~3) of the 4-node model and elements C8, NC8-QH, and NC8-A2 of the 8-node model are selectively checked if the nonconforming Mindlin plate elements which do not pass the Irons' patch test can pass the weak patch test. For the weak patch tests, the successively refined meshes with distorted shapes, i.e., 4x4, 8x8, 12x12, and 16x16 meshes for 4-node element models and 2x2, 4x4, 6x6, and 8x8 meshes for 8-node models as shown in Fig. 8, are constructed for thick and thin plates and are tested under the pure bending and pure shearing conditions as shown in Fig. 4 to see if a constant

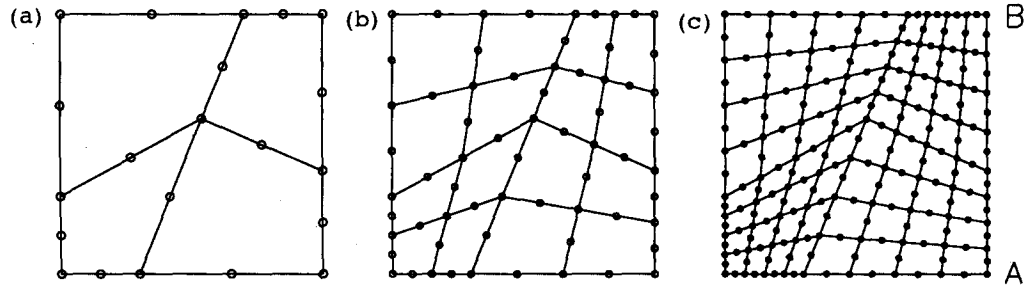

Fig. 8 Mesh sequences for weak patch test (8-node element); (a) 2x2 mesh, (b) 4x4 mesh, (c) 8x8 mesh.

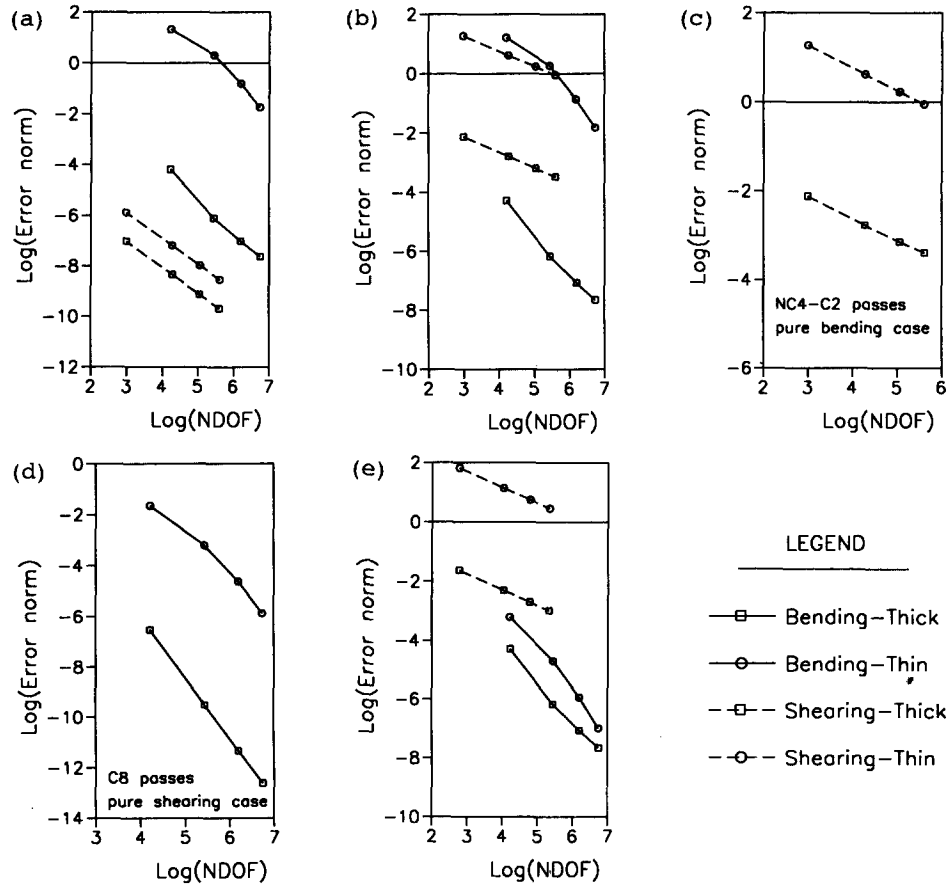

Fig. 9 Error in energy norm versus number of degrees of freedom from weak patch test; (a) NC4-B0, (b) NC4-B2, (c) NC4-C2, (d) C8, (e) NC8-QH.

strain state (or nearly constant state) can be obtained as the mesh is refined.

One natural, convenient, and frequently used mathematical tool to measure the finite element approximation error is the energy norm which measures the strain energy of errors and is defined as

$$\|e\|_E^2 = \int_\Omega (\sigma_{EXACT} - \sigma_{FEM})^T \boldsymbol{D}^{-1} (\sigma_{EXACT} - \sigma_{FEM}) d\Omega \tag{14}$$

For convergence proof, the error norm should decrease with the mesh refinement. The errors in energy norm with the progressively refined meshes for weak patch tests are plotted on the log-log scale in Fig. 9 for some selected elements NC4-B0, NC4-B2, NC4-C2, C8 and NC8-QH. It is recognized that the errors in energy norm decrease in general monotonically with mesh refinement for all the selected elements. This means that the magnitudes of stress error decrease and each element can gradually represent the constant strain state as the mesh is refined. Thus, these elements are expected to be convergent and to pass the weak patch test even though they do not pass the classical Irons' patch tests.

In the weak patch test, the convergence of displacements are also checked and listed in Tables 3 through 6. From Tables 3(a) and 4(a), all of the nonconforming 4-node elements are shown

to converge to the exact solution for both thick and thin plates in pure bending condition while the conforming C4 element gives very poor result in thin plate. For the pure shearing case in thick plate, the NC4-B0 shows a fast convergence and NC4-B2 are a little slow convergent

Table 3 Displacements for thick plate from weak patch test (4-node)
(a) Pure bending case

Element	Point	4x4	8x8	12x12	16x16	Comment
C4	A	0.596247E−03	0.121139E−02	0.153874E−02	0.170761E−02	convergent
	B	0.571122E−03	0.117822E−02	0.151402E−02	0.169031E−02	
NC4-B0	A	0.193199E−02	0.199317E−02	0.199788E−02	0.199899E−02	convergent
	B	0.192555E−02	0.199702E−02	0.200013E−02	0.200036E−02	
NC4-B2	A	0.193380E−02	0.199314E−02	0.199787E−02	0.199898E−02	convergent
	B	0.192826E−02	0.199705E−02	0.200013E−02	0.200036E−02	
NC4-C2	A	Exact	Exact	Exact	Exact	passed Irons' test
	B					
Exact				0.200000E-02		

(b) Pure shearing case

Element	Point	4x4	8x8	12x12	16x16	Comment
C4	A	Exact	Exact	Exact	Exact	passed Irons' test
	B					
NC4-B0	A	0.105207E−03	0.104304E−03	0.104136E−03	0.104076E−03	convergent
	B	0.105324E−03	0.104337E−03	0.104150E−03	0.104085E−03	
NC4-B2	A	0.258952E−03	0.144289E−03	0.122034E−03	0.114171E−03	0.1098E−03*
	B	0.242194E−03	0.139303E−03	0.119785E−03	0.112901E−03	0.1091E−03*
NC4-C2	A	0.349927E−03	0.235018E−03	0.212626E−03	0.204693E−03	0.2046E−03*
	B	0.367736E−03	0.264852E−03	0.245347E−03	0.238492E−03	0.2347E−03*
Exact				0.104000E−03		

*: Extrapolated displacements by Aitken's method (Atkinson 1978) based on 8x8, 12x12 and 16x16 mesh.

Table 4 Displacements for thin plate from weak patch test (4-node)
(a) Pure bending case

Element	Point	4x4	8x8	12x12	16x16	Comment
C4	A	0.111131E−01	0.438248E−01	0.928821E−01	0.153651E+00	slow
	B	0.967834E−02	0.376003E−01	0.810950E−01	0.136543E+00	convergent
NC4-B0	A	0.114118E+01	0.180034E+01	0.194216E+01	0.197954E+01	convergent
	B	0.852875E+00	0.167161E+01	0.190498E+01	0.196668E+01	
NC4-B2	A	0.144411E+01	0.181442E+01	0.194387E+01	0.197987E+01	convergent
	B	0.990715E+00	0.167808E+01	0.190607E+01	0.196694E+01	
NC4-C2	A	Exact	Exact	Exact	Exact	passed Irons' test
	B					
Exact				0.200000E+01		

(b) Pure shearing case

Element	Point	4x4	8x8	12x12	16x16	Comment
C4	A B	Exact	Exact	Exact	Exact	passed Irons' test
NC4-B0	A B	0.105207E−02 0.105324E−02	0.104304E−02 0.104337E−02	0.104136E−02 0.104150E−02	0.104076E−02 0.104085E−02	convergent
NC4-B2	A B	0.128995E+00 0.128463E+00	0.369106E−01 0.346115E−01	0.180219E−01 0.161371E−01	0.107892E−01 0.956885E−02	0.6301E−02* 0.5944E−02*
NC4-C2	A B	0.130368E+00 0.130089E+00	0.379730E−01 0.360659E−01	0.190115E−01 0.175296E−01	0.117704E−01 0.109356E−01	0.7296E−02* 0.7294E−02*
Exact				0.104000E−02		

*: Extrapolated displacements by Aitken's method (Atkinson 1978) based on 8x8, 12x12 and 16x16 mesh.

Table 5 Displacements for thick plate from weak patch test (8-node)
(a) Pure bending case

Element	Point	2x2	4x4	6x6	8x8	Comment
C8	A B	0.199769E-02 0.199787E-02	0.199994E-02 0.199994E-02	0.199999E-02 0.199999E-02	0.200000E-02 0.200000E-02	converged
NC8-QH	A B	0.199994E-02 0.199713E-02	0.199993E-02 0.199994E-02	0.199999E-02 0.199999E-02	0.200000E-02 0.200000E-02	converged
NC8-A2	A B	0.199832E-02 0.199745E-02	0.199994E-02 0.199994E-02	0.199999E-02 0.199999E-02	0.200000E-02 0.200000E-02	converged
Exact				0.200000E−02		

(b) Pure shearing case

Element	Point	2x2	4x4	6x6	8x8	Comment
C8	A B	Exact	Exact	Exact	Exact	passed Irons' test
NC8-QH	A B	0.631742E-03 0.534365E-03	0.238282E-03 0.217938E-03	0.163706E-03 0.155325E-03	0.137651E-03 0.133071E-03	0.1236E-03* 0.1208E-03*
NC8-A2	A B	0.551224E-03 0.540539E-03	0.232362E-03 0.218884E-03	0.162674E-03 0.155675E-03	0.137331E-03 0.133225E-03	0.1228E-03* 0.1209E-03*
Exact				0.104000E−03		

*: Extrapolated displacements by Aitken's method (Atkinson 1978) based on 4x4, 6x6 and 8x8 mesh.

but the NC4-C2 converged to an overestimated displacement as noticed in Table 3(b). In the thin plate under pure shearing condition, the NC4-B0 is convergent but both NC4-B2 and NC4-C2 elements overestimate the displacements as shown in Table 4(b).

In the case of 8-node elements, the conforming and nonconforming elements, C8, NC8-A2, and NC8-QH show a fast convergence for both the thick and thin plates in the pure bending condition as shown in Table 5(a) and Table 6(a), in spite that these elements did not pass the Irons' patch test for the pure bending case. For the pure shearing case, NC8-A2 and NC8-

Table 6 Displacements for thin plate from weak patch test (8-node)
(a) Pure bending case

Element	Point	2x2	4x4	6x6	8x8	Comment
C8	A	0.199012E+01	0.199921E+01	0.199990E+01	0.199998E+01	convergent
	B	0.199704E+01	0.199952E+01	0.199991E+01	0.199998E+01	
NC8-QH	A	0.200038E+01	0.200001E+01	0.200000E+01	0.200000E+01	convergent
	B	0.199637E+01	0.199982E+01	0.199997E+01	0.199999E+01	
NC8-A2	A	0.199644E+01	0.199961E+01	0.199993E+01	0.199999E+01	convergent
	B	0.199540E+01	0.199971E+01	0.199992E+01	0.199998E+01	
Exact				0.200000E−01		

(b) Pure shearing case

Element	Point	2x2	4x4	6x6	8x8	Comment
C8	A	Exact	Exact	Exact	Exact	passed Irons' test
	B					
NC8-QH	A	0.524373E+00	0.133408E+00	0.595230E−01	0.339505E−01	0.2041E−01*
	B	0.431528E+00	0.112776E+00	0.511604E−01	0.293287E−01	0.1735E−01*
NC8-A2	A	0.417685E+00	0.107929E+00	0.514414E−01	0.311971E−01	0.1989E−01*
	B	0.405881E+00	0.107325E+00	0.500442E−01	0.290636E−01	0.1694E−01*
Exact				0.104000E−02		

*: Extrapolated displacements by Aitken's method (Atkinson 1978) based on 4x4, 6x6 and 8x8 mesh.

QH elements which did not pass the Irons' patch test for the pure shearing case show convergent behaviors in case of thick plate as shown in Table 5(b), but these elements tend to overestimate the displacement in case of thin plate as shown in Table 6(b) like the NC4-B2 and NC4-C2 of 4-node element. However, these elements should not be simply discarded since these elements are shown to be practically useful as will be seen in the following benchmark numerical problems.

For the pure twisting case, the same results are obtained for the elements tested.

Summaries of the patch tests along with the weak patch tests for 4-node and 8-node nonconforming elements are given in Table 1 and Table 2, respectively.

5. Convergence tests

What is meant by convergence in the finite element approximation is that the approximation should approach to the exact solution when the size of elements h tends to zero. To check the convergence of nonconforming Mindlin plate elements listed in Tables 1 and 2, benchmark analyses with square and circular plates have been performed. The plate elements selected for the convergence tests can be grouped into three categories; (1) those which pass the Irons' tests(NC 8-DS), (2) those which do not pass the Irons' tests but pass the weak patch tests(NC4-B0, C8), and (3) those which do not pass fully both the Irons' tests and weak patch tests(NC4-B2, NC4-C2, NC8-QH).

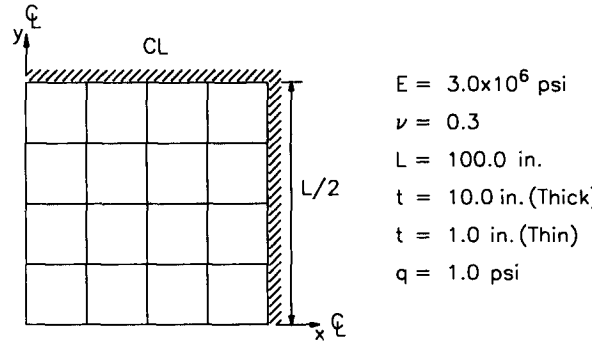

Fig. 10 Square plate test model and material properties.

Table 7 Normalized displacements for thick square plate (L/t= 10): 4-node model

Element	2x2	4x4	8x8	16x16	24x24
NC4-B0	0.88710	0.98586	0.99815	1.00052	1.00093
NC4-B2	1.02360	1.02346	1.00772	1.00292	1.00200
NC4-C2	1.09714	1.14171	1.14956	1.15165	1.15206

Table 8 Normalized displacements for thin square plate (L/t= 100): 4-node model

Element	2x2	4x4	8x8	16x16	24x24
NC4-B0	0.09560	0.63464	0.96492	0.99820	1.00033
NC4-B2	0.12092	0.67208	0.97668	1.00121	1.00167
NC4-C2	0.85538	0.97956	0.99970	1.00239	1.00278

Table 9 Normalized displacements for thick square plate (L/t= 10): 8-node model

Element	1x1	2x2	4x4	8x8	12x12
C8	1.15123	0.99740	1.00163	1.00126	1.00125
NC8-DS	0.99717	0.98141	0.99561	0.99986	1.00119
NC8-QH	1.28173	1.00122	1.00207	1.00137	1.00128

5.1. Square plate

One quarter of a thick or thin square plate under a uniform load is modeled with a clamped boundary. For the model shown in Fig. 10, the successively refined meshes were constructed and the convergence of each solution is checked. The normalized displacements to the exact solutions of thick and thin plate (Hinton and Huang 1986, Timoshenko and Woinowsky-Krieger 1959) are listed in Table 7 and 8 for 4-node model, and Table 9 and 10 for 8-node model.

As noticed in Table 7 through Table 10, most elements converge to the exact solution except the NC4-C2 element which converges to a overestimated displacement in case of thick plate

Table 10 Normalized displacements for thin square plate (L/t= 100): 8-node model

Element	1x1	2x2	4x4	8x8	12x12
C8	1.21819	0.62102	0.99355	1.00102	1.00108
NC8-DS	0.26145	0.95268	1.00001	1.00106	0.99796
NC8-QH	1.45643	1.00117	1.00057	1.00106	1.00109

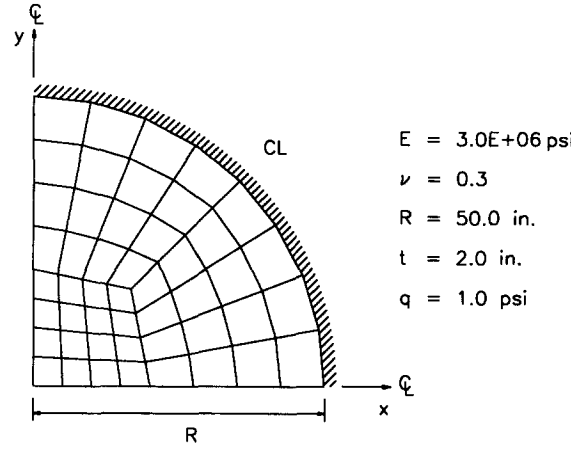

Fig. 11 Circular plate test model and material properties.

Table 11 Normalized displacements to thin plate solution for uniformly loaded clamped circular plate (2R/t=50)

(a) 4-node element model

Element	NEL=3	NEL=12	NEL=48	NEL=192
NC4-B0	0.47754	0.89274	0.99350	1.00522
NC4-B2	0.65106	0.93594	1.00425	1.00793
NC4-C2	0.90441	0.98829	1.00848	1.01330

(b) 8-node element model

Element	NEL=1	NEL=3	NEL=12	NEL=48
C8	0.32552	0.98905	1.00595	1.00731
NC8-DS	0.77279	1.00932	1.00807	1.00732
NC8-QH	0.83977	1.02307	1.00740	1.00732

(Table 7) as did in the weak patch test for the pure shearing situation in thick plate (Table 3(b)). In the thick plate, since the transverse displacement due to the shear deformation is no longer negligible, this type of element should not be seriously considered for further study. The NC4-B2 and NC4-C2 elements also overestimated the displacements for the pure shearing situation in the thin plate as did in the weak patch test (Table 4(b)). These elements, however, show good convergent behaviors in the analysis of thin square plates as shown in Table 8. This is because the effect of shear deformation diminishes as the plate thickness becomes thinner.

The NC8-QH element overestimates the displacements for the pure shearing situation in thin plate while slightly overestimates it in thick plate in the weak patch test (Tables 5(b) and 6(b)). This element, however, shows good convergent performance in the thin plate as the plate thickness decreases and the shear effect diminishes (Table 10). The NC8-QH element does not lock in extremely thin plate even for the distorted mesh (Kim and Choi 1992).

5.2. Circular plate

To check the performance of the elements under consideration with distorted meshes, the circular plate is analysed. One quarter of moderately thin circular plate under a uniform load was modeled with a clamped boundary condition. The geometry and material properties used and mesh shapes are shown in Fig. 11. The normalized central displacements to the thin plate solution (Timoshenko and Woinowsky-Krieger 1959) are listed in Table 11. It is noticed that all the nonconforming 4-node and 8-node elements converge to the exact solution rapidly. Similar to the analysis of the thick square plate, NC4-C2 tends to slightly overestimate the displacement compared with other elements.

6. Conclusions

In the paper, the classical Irons' patch tests and converegence characteristics of the nonconforming Mindlin plate elements are investigated. The clues to pass the Irons' patch tests are presented and it is shown that some of the nonconforming elements can pass all the patch tests even though they violate the interelement conformity by addition of incompatible higher modes to the original conforming modes. Also, it is noticed that many nonconforming elements partially pass the tests if they do not fully pass the test, e.g., NC4-Ci(i=0~3) series elements pass the test for the pure bending case but do not pass for the pure shearing case.

It was recognized from the benchmark numerical tests that the conforming element C8 and nonconforming element NC4-B0 which do not pass Irons' patch test but pass all the cases of weak patch tests, and the nonconforming elements NC4-B2 and NC8-QH which do not pass the Irons' patch tests and also pure shearing case of weak patch test in thin plate, are still convergent. The conforming element C4 which failed to pass the weak patch test for the pure bending in thin plate did not converge to the exact solution, and the nonconforming element NC4-C2 which failed to pass the weak patch test for the pure shearing in thick plate converged to a rather overestimated solution. Thus, for the converegence proof of a Mindlin plate element which does not pass the Irons' patch test, it is necessary to pass at least weak patch tests suggested in the paper for the thick and thin plate (or extremely thin plate if no shear locking is desired) under pure bending and pure shearing conditions. An exception for the requirement to pass the weak patch test is the pure shearing case in thin plate where the effects of shear deformation becomes negligible as the thickness of plate is reduced.

It will be concluded that the Irons' patch test should be considered as the sufficient condition but not the necessary condition for the nonconforming Mindlin plate element to prove its convergence, since it is observed that not only those elements which pass the Irons' patch test converge to the exact solution, but also some other elements which do not pass the Irons' patch test exactly may still be convergent.

In case of 4-node element, the NC4-Bi(i=0~3) series nonconforming elements which did not pass the Irons' patch tests but passed the weak patch tests are more favorable for practical use than the NC4-Ci(i=0~3) series nonconforming elements which partially passed the Irons' patch test but overestimated the displacements in the analysis of thick plate. In the case of 8-node element, the nonconforming elements NC8-DS and NC8-QH are favorable for the practical use because the former passes the Irons' patch test and shows a faster convergent behavior and the latter which did not pass the Irons' patch tests but passed the weak patch tests shows the fastest convergence and has been known not to exhibit shear locking for the extremely thin plate.

References

Atkinson, K. (1978), *An Introduction to Numerical Analysis*, John Wiley & Sons, New York.

Bathe, K.J. (1982), *Finite Element Procedures in Engineering Analysis*, Prentice-Hall, New Jersey.

Bazeley, G.P., Cheung, Y.K., Irons, B.M. and Zienkiewicz, O.C. (1966), "Triangular elements in plate bending. Conforming and nonconforming solutions," *Proc. 1st Conf. Matrix Methods in Structural Mechanics*, AFFDL-TR-CC-80, Wright Patterson A.F. Base, Ohio, 547-576.

Belytshko, T. and Lasly, D. (1988), "A fractal patch test," *Int. J. Numer. Methods Eng.*, **26**, 2199-2210.

Choi, C.K. and Kim, S.H. (1989), "Coupled use of reduced integration and nonconforming modes in quadratic Mindlin plate element," *Int. J. Numer. Methods Eng.*, **28**, 1909-1928.

Choi, C.K. and Park, Y.M. (1989), "Nonconforming transition plate bending elements with variable mid-side nodes," *Comp. Struct.*, **32**, 295-304.

Choi, C.K. and Schnobrich, W.C. (1975), "Nonconforming finite element analysis of shells", *J. Eng. Mech. Div. ASCE*, **101**, 447-464.

Donea, J., and Lamain, L.G. (1987), "A modified representation of transverse shear in Co quadrilateral plate elements", *Comput. Meth. in Appl. Mech. and Eng.*, **63**, 183-207.

Hinton, E. and Huang, H.C. (1986), "A family of quadrilateral Mindlin plate elements with substitute shear strain fields," *Comp. Struct.*, **23**, 409-431.

Hughes, T.J.R. and Cohen, M. (1978), "The heterosis finite element for plate bending," *Comp. Struct.*, **9**, 445-450.

Irons, B.M. and Razzaque, A. (1972), "Experience with the patch test for convergence of finite element methods," *Math. Foundations of the Finite Element Method* (Ed. A. K. Aziz), Academic Press, 557-587.

Kim, S.H. and Choi, C.K. (1992), "Improvement of quadratic finite element for Mindlin plate bending," *Int. J. Numer. Methods Eng.*, **34**, 197-208.

Pugh, E.D.L., Hinton, E. and Zienkiewicz, O.C. (1978), "A study of quadrilateral plate bending elements with reduced integration," *Int. J. Numer. Methods Eng.*, **12**, 1059-1079.

Razzaque, A. (1986), "The patch test for elements," *Int. J. Numer. Methods Eng.*, **22**, 63-71.

Stummel, F. (1980), "The limitations of the patch test," *Int. J. Numer. Methods Eng.*, **15**, 177-188.

Taylor, R.L., Beresford, P.J. and Wilson, E.L. (1976), "A nonconforming element for stress analysis," *Int. J. Numer. Methods Eng.*, **10**, 1211-1219.

Taylor, R.L., Simo, J.C., Zienkiewicz, O.C. and Chan, A.C.H. (1986), "The patch test-A condition for assessing FEM converegence," *Int. J. Numer. Methods Eng.*, **22**, 39-62.

Timoshenko, S.P. and Woinowsky-Krieger, S. (1959), Theory of Plates and Shells, 2nd ed., McGraw-Hill, New York.

Verma, A. and Melosh, R.J. (1987), "Numerical tests for assessing Finite Element model convergence," *Int. J. Numer. Methods Eng.*, **24**, 843-857.

Zienkiewicz, O.C., Taylor, R.L. and Too, J.M. (1971), "Reduced integration technique in general analysis of plates and shells," *Int. J. Numer. Methods Eng.*, **3**, 275-290.

Appendix

Let the material rigidity matrices, $\boldsymbol{D}_b$ and $\boldsymbol{D}_s$ in Eq. (3) denote as follows.

$$\boldsymbol{D}_b = \begin{bmatrix} D_1 & D_{12} & 0 \\ D_{21} & D_2 & 0 \\ 0 & 0 & D_3 \end{bmatrix} \tag{A.1}$$

$$\boldsymbol{D}_s = \begin{bmatrix} G_1 & 0 \\ 0 & G_2 \end{bmatrix} \tag{A.2}$$

First, when the nonconconforming mode $\bar{N}_5$ is added into rotational degrees of freedom, the $\boldsymbol{K}_{cn}(3n\times 2$ matrix) in Eq. (6) is obtained by integrating the following matrix.

$$\boldsymbol{B}^T\boldsymbol{D}\bar{\boldsymbol{B}} = \begin{bmatrix} N_{i,x}G_1\bar{N}_5 & N_{i,y}G_2\bar{N}_5 \\ N_{i,x}D_1\bar{N}_{5,x} & N_{i,x}D_{12}\bar{N}_{5,y} \\ +N_{i,y}D_3\bar{N}_{5,y} & +N_{i,y}D_3\bar{N}_{5,x} \\ +N_iG_1\bar{N}_5 & \\ N_{i,y}D_{21}\bar{N}_{5,x} & N_{i,y}D_2\bar{N}_{5,y} \\ +N_{i,x}D_3\bar{N}_{5,y} & +N_{i,x}D_3\bar{N}_{5,x} \\ & +N_iG_2\bar{N}_5 \end{bmatrix} \tag{A.3}$$

where, comma denotes partial differential and i varies from 1 to n.

Secondly, when the nonconconforming mode $\bar{N}_5$ is added into transverse displacement, the $\boldsymbol{K}_{cn}(3n\times 1$ matrix) is obtained by integrating the following matrix.

$$\boldsymbol{B}^T\boldsymbol{D}\bar{\boldsymbol{B}} = \begin{bmatrix} N_{i,x}G_1\bar{N}_{5,x}+N_{i,y}G_2\bar{N}_{5,y} \\ N_iG_1\bar{N}_{5,x} \\ N_iG_2\bar{N}_{5,y} \end{bmatrix} \tag{A.4}$$